

Available online at www.sciencedirect.com

jmr&t
Journal of Materials Research and Technology
www.jmrt.com.br



Original Article

Kinetic study and synergistic interactions on catalytic CO₂ gasification of Sudanese lower sulphur petroleum coke and sugar cane bagasse

Elbager M.A. Edreis^{a,*}, Xiao Li^b, Chaofen Xu^b, Hong Yao^b

^a Department of Mechanical Engineering, Faculty of Engineering, University of Blue Nile, Roseires, Sudan

^b State Key Laboratory of Coal Combustion, Huazhong University of Science and Technology, Wuhan 430074, China

ARTICLE INFO

Article history:

Received 28 January 2016

Accepted 12 September 2016

Available online xxx

Keywords:

Catalytic CO₂ gasification

Petroleum coke

Reactivity

Activation energy

Synergistic interactions

ABSTRACT

In this study the effects of iron chloride (FeCl₃) on the CO₂ gasification kinetics of lower sulphur petroleum coke (PC) and sugar cane bagasse (SCB) via thermogravimetric analyser (TGA) were investigated. The FeCl₃ loading effects on the thermal behaviour and reactivity of CO₂ gasification of PC were studied. The possible synergistic interaction between the PC and SCB was also examined. Then the homogeneous model or first order chemical reaction (O₁) and shrinking core models (SCM) or phase boundary controlled reactions (R₂ and R₃) were employed through Coats–Redfern method in order to detect the optimum mechanisms for the catalytic CO₂ gasification, describe the best reaction behaviour and determine the kinetic parameters. The results showed that the thermal behaviour of PC is significantly affected by the FeCl₃ loading. Among various catalyst loadings, the addition of 7 wt% FeCl₃ to PC leads to improve the PC reactivity up to 39% and decrease the activation energy up to 22%. On the other hand, for char gasification stage of SCB and blend, the addition 5 wt% FeCl₃ improved their reactivities to 18.7% and 29.8% and decreased the activation energies to 10% and 17%, respectively. The synergistic interaction between the fuel blend was observed in both reaction stages of the blend and became more significant in the pyrolysis stage. For all samples model R₂ shows the lowest values of activation energy (E) and the highest reaction rates constant (k). Finally, model R₂ was the most suitable to describe the reactions of non-catalytic and catalytic CO₂ gasification.

© 2016 Brazilian Metallurgical, Materials and Mining Association. Published by Elsevier Editora Ltda. This is an open access article under the CC BY-NC-ND license (<http://creativecommons.org/licenses/by-nc-nd/4.0/>).

1. Introduction

Developing countries suffer from the problem of over consumption of energy. Most likely, the solution to meet the

energy needs in the future will emanate from the combination of energy resources such as petroleum coke (PC) and biomass. PC is a carbonaceous solid derived from oil refinery units consisting of polycyclic aromatic hydrocarbons with low hydrogen content [1,2]. The efficient use of PC for energy

* Corresponding author.

E-mail: bager146@gmail.com (E.M. Edreis).

<http://dx.doi.org/10.1016/j.jmrt.2016.09.001>

2238-7854/© 2016 Brazilian Metallurgical, Materials and Mining Association. Published by Elsevier Editora Ltda. This is an open access article under the CC BY-NC-ND license (<http://creativecommons.org/licenses/by-nc-nd/4.0/>).

resource is strongly promoted [3]. Bayram et al. [4] reported that one tonne of crude oil produces approximately 31 kg of PC. PC is mainly used as fuel or for manufacturing dry cells and electrodes [2]. The most important feature that makes PC a very good fuel and attractive energy resource for power generation in gasification is related to its low price, high heating value ($>32 \text{ MJ kg}^{-1}$), high carbon ($>90 \text{ wt\%}$) and low ash content [1,2,5,6]. Therefore, the low reactivity and high-sulphur content are its main disadvantages [6–8]. However, the main advantage of Sudanese PC is its lower sulphur. This is an important issue for clean energy generation [1,2].

Bagasse is a fibrous residue of the cane stalk after crushing and extracting the juice, which consists of approximately 26.6–54.3% cellulose, 22.3–29.7% hemicelluloses, 14.3–24.45% lignin and about 2–4% ash on a dry basis [1,2,9–12]. In comparison to other agricultural residues, bagasse is considered as a rich solar energy reservoir due to its very high yields. Moreover, bagasse is a cheap, plentiful and low emission fuel. In addition, harvesting chemical energy from bagasse is attractive. The combustion/gasification of sugarcane produces the same amount of CO_2 as it is consumed during its growth, so it is carbon neutral [1,9]. By implementing thermo-chemical upgrading of bagasse, the energy efficiency can be significantly increased, resulting in saving energy and surplus products [1,2,11,13].

Gasification is a clean, efficient, promising technology and an attractive option to provide high quality fuel gases [1–3]. In order to obtain high quality fuel gases, high reactivity and high conversion rate of char are essential. The char conversion directly depends on the reactivity of char with gasifying agents (H_2O , CO_2 , etc.). However, low reactivity remains an important problem for utilising PC through gasification, due to compactness of carbon structure as well as its low volatile behaviour and ash content [3]. Several authors have reported that gasification reactivity can be significantly enhanced by different metal compound catalysts (K, Na, Ca, Mg, Ba, Fe, Ni, etc.) [3,14,15]. Catalytic gasification is one of the main techniques used to improve the gasification reactivity due to its efficiency, availability, and low cost [3,14,16]. The addition of catalysts, such as alkali (K), alkaline earth (Ca) and transition metal (Fe), can significantly improve the gasification reactivity of PC [3]. Considering these events, it should be an important evidence to study the effects of catalysts on CO_2 gasification of Sudanese PC.

Iron compounds are potential gasification catalysts due to their abundance, low cost, and environmentally friendliness. Several iron compounds have been tested to catalyse coal gasification and their effects on coal pyrolysis and char gasification as well as tar formation during the whole coal gasification process have been studied [14,17]. Li et al. [3] studied the catalytic effects of FeCl_3 , CaCl_2 , KCl , K_2CO_3 , K_2SO_4 , KAC ($\text{CH}_3 \text{ COOK}$) and KNO_3 during steam gasification of PC. They have found that the gasification of PC was inefficient at temperature $<1000^\circ\text{C}$. However, with the addition of catalysts the efficiency greatly improved. In particular, with the addition of K_2CO_3 , gasification was quickly completed in 10 min and the final temperature was about 900°C . Zhou et al. [18] investigated the catalytic effect of iron species (FeCl_3 , $\text{Fe}(\text{NO}_3)_3$, FeSO_4) on CO_2 gasification of PC using TGA. They found that the catalytic activity of iron species followed

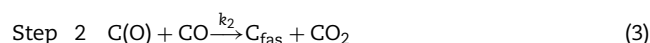
the order of $\text{FeCl}_3 > \text{Fe}(\text{NO}_3)_3 > \text{FeSO}_4$. Lahijani et al. [19] studied the catalytic effect of iron species ($\text{Fe}(\text{NO}_3)_3$, FeCl_3 and $\text{Fe}_2(\text{SO}_4)_3$) on CO_2 gasification reactivity of oil palm shell char. They reported the catalytic effect of iron species on promoting reactivity of char was considerable in the order of $\text{Fe}(\text{NO}_3)_3 > \text{FeCl}_3 > \text{Fe}_2(\text{SO}_4)_3$.

The catalytic mechanism of the gasification reaction could be explained by the reaction of some active intermediate sites in the gasification process such as $\text{C}(\text{O})$ (active intermediates of carbon matrix) and $\text{M}-\text{C}-\text{O}$ (active intermediates of carbon matrix with catalyst) with the gasification agent CO_2 . When catalyst-PC or SCB or blend mixture was heated, the metal cations were combined with the edge C atom of char surface to form the intermediate $\text{M}-\text{O}-\text{C}$ (where M is a metal) in the CO_2 atmosphere. Meanwhile, the distribution of the electron cloud in C atom of char surface was changed with the structure of $\text{M}-\text{O}-\text{C}$. Consequently, the intensity of $\text{C}-\text{C}$ was weakened. As a result, the concentration of the intermediate $\text{C}(\text{O})$ and $\text{M}-\text{C}-\text{O}$ increased rapidly, leading to a rapid increase in the gasification reactivity [3]. The gasification of char in carbon dioxide is popularly known as the Boudouard reaction (Eq. (1)).



Di Blasi et al. [20] describes the Boudouard reaction through the following steps:

In the first step, CO_2 dissociates at a carbon-free active site (C_{fas}), releasing carbon monoxide and forming a carbon-oxygen surface complex, $\text{C}(\text{O})$. This reaction can move in the opposite direction as well, forming a carbon active site and CO_2 in the second step. In the third step, the carbon-oxygen complex produces a molecule of CO .



where k_i is the rate of the reaction.

The formation of active intermediates from char sample and gasifying agent was essential for gasification to occur. Therefore, the contact area between char and CO_2 was critical for gasification reactivity [3].

The previous studies revealed that a synergetic interaction could be expected in the co-processes of biomass and coal or PC because of the high thermochemical reactivity and high volatile matter content of biomass [2]. The synergistic interaction during non-catalytic gasification of the combining fuels such as coal or PC with biomass has been investigated by several authors [1,2,6,21,22]. However, the synergistic interaction between the Sudanese low sulphur PC and SCB during CO_2 catalytic gasification has not been reported yet. In spite of significant on-going research of the thermal conversion technologies such as pyrolysis and gasification for production of energy and fuels, there is no information about catalytic activity of iron species in the Sudanese low sulphur PC. This remains a relatively unexplored area of research. Based on these points, the aims of this study are:

Table 1 – Fuels properties.

Sample	Proximate analysis (db %)				Ultimate analysis (db %)					Lower heating value (LHV) (MJ kg ⁻¹ , db)		
	Ash	VM	FC		C	H	N	S	O ^a			
PC	2.01	10.83	86.52		92.09	3.76	1.66	1.08	3.03			35.52
SCB	4.759	83.01	12.23		46.95	6.06	0.13	0.08	42.44			16.30
Ash analysis												
Oxide	Na ₂ O	MgO	Al ₂ O ₃	SiO ₂	SO ₃	K ₂ O	CaO	Fe ₂ O ₃	V ₂ O ₅	Ni ₂ O ₃	TiO ₂	P ₂ O ₅
PC	2.19	1.25	2.24	1.19	40.7	3.12	44.23	2.33	0.11	1.09	0.62	0.94
SCB	0.70	4.41	17.04	54.62	1.52	4.41	7.54	7.32	0.06	0.02	0.87	1.41
db, dry ash basis.												
^a Calculated by (difference).												

db, dry ash basis.

^a Calculated by (difference).

- (1) To study the effect of iron chloride (FeCl₃) on the kinetic behaviour and reactivity of the Sudanese low sulphur PC and SCB during CO₂ gasification via thermogravimetric analyser (TGA).
- (2) To investigate the possible synergistic interactions between the Sudanese low sulphur PC and SCB during catalytic CO₂ gasification.
- (3) To observe the optimum mechanisms for the catalytic CO₂ gasification of the fuels and describe the best reactive behaviour.
- (4) To estimate the kinetic parameters by applying homogeneous model (HM) or first order chemical reaction (O₁) and shrinking core models (SCM) or phase boundary controlled reactions (R₂ and R₃) through Coats–Redfern method.

2. Experimental

2.1. Materials

Petroleum coke (PC) and sugar cane bagasse (SCB) used in this study were obtained from Sudan. The samples were ground and sieved to particle sizes ranging from 53 to 100 μm. The fuel mixtures were mixed in appropriate proportions and homogenised at the PC to SCB ratio of (1:1). The proximate analysis of samples was carried out using thermogravimetric analyser (TGA-2000, Navas Instruments, Spain), while ultimate analysis was conducted by using elemental analyser (Euro-CA 3000, HEKA tech, Italy). The ash component was analysed with an X-fluorescence probe (XRF) technique. The relevant analyses data are presented in Table 1.

2.2. Methods

2.2.1. Loading of catalyst

The iron chloride hexa hydrate (FeCl₃·6H₂O) was introduced into PC, SCB and blend by wet impregnation method. The aqueous solutions of FeCl₃ were prepared by dissolving quantitative amounts of FeCl₃·6H₂O in deionized water. Five grams of PC or SCB powder was impregnated in 80 mL of the prepared aqueous solution and stirred for 24 h at room temperature. Afterwards, the mixtures were dried at 105 °C.

Various catalyst loadings were achieved by changing the concentration of FeCl₃ (0–9 wt%) in the solution [23,24].

2.2.2. The catalytic and non-catalytic CO₂ gasification experiments

The catalytic and non-catalytic CO₂ gasification of the PC, SCB and blend were carried out in the thermogravimetric analyser (TGA, NETZSCHSTA 449/F3) under non-isothermal conditions. High purity CO₂ was used as gasification agent at the flowing rate of 100 mL min⁻¹, about (9–10 mg) of sample was used in each experiment. The samples were heated up to 1300 °C at a constant heating rate of 10 °C min⁻¹.

2.2.3. Synergistic interactions

In order to understand if there is the interaction between the PC and SCB, the theoretical DTG curves were calculated by Eq. (5) based on experiment data of PC and SCB collected at the same temperature. The curves represented the sum of the individual component's behaviour in the blends. In this study 5 wt% FeCl₃ was loaded into the blend (PC:SCB) or (1:1) which was used to investigate the possible synergistic interactions between the PC and SCB during catalytic CO₂.

$$\frac{dw}{dt} = x_{PC} \left(\frac{dw}{dt} \right)_{PC} + x_{SCB} \left(\frac{dw}{dt} \right)_{SCB} \quad (5)$$

where dw/dt , $(dw/dt)_{PC}$, and $(dw/dt)_{SCB}$ are the normalised rates of the weight loss of the mixture fuels, PC and SCB, respectively, while x_{PC} and x_{SCB} are the mass fractions of PC and SCB in the blend, respectively.

2.2.4. Reactivity measurements

CO₂ gasification reactivity of samples was calculated using TGA analysis data.

The thermogravimetric experiment results were expressed as a function of conversion (x), which is defined as [18,19]:

$$x = \frac{w_i - w_t}{(w_i - w_c - w_f)} \times 100 \quad (6)$$

where w_i is the initial sample mass (mg), w_t refer to sample mass at given time t (min), w_f is the final sample mass at the end of gasification (mg), and w_c is catalytic mass (mg).

Table 2 – Expressions of $f(x)$ and $g(x)$ for the kinetic model functions usually employed for solid-state reactions ([2,2]9).

Model	Symbol	$f(x)$	$g(x)$
Chemical reaction (HM)			
First-order	O_1	$(1-x)$	$-\ln(1-x)$
Phase boundary controlled reactions (SCM)			
Two dimensions (Contracting Cylinder)	R_2	$2(1-x)^{1/2}$	$1-(1-x)^{1/2}$
Three dimensions (Contracting Sphere)	R_3	$3(1-x)^{2/3}$	$1-(1-x)^{1/3}$

In order to quantify the gasification reactivity of samples, the R_i is used as reactivity index, which is defined as follows [23,25]:

$$R_i = \frac{0.5}{t_{0.5}} \quad (7)$$

where $t_{0.5}$ is the time required to reach the carbon conversion of 50% per minute.

2.2.5. Kinetics study

The kinetic parameters such as activation energy (E), a pre-exponential factor (A) and reaction rate constant (k) were obtained by applying homogeneous model (HM) or first order chemical reaction (O_1) and shrinking core models (SCM) or Phase boundary controlled reactions (R_2 and R_3) through Coats-Redfern method based on Arrhenius's equation.

In order to gain some insight into the reaction mechanisms on a thermal conversion process, the data were fitted to a series of solid-state mechanisms. A well-established method of data analysis assumes the general rate dx/dt , Eq. (8).

$$\frac{dx}{dt} = kf(x) \quad (8)$$

where k is rate constant (min^{-1}) and $f(x)$ refers to the reasonable model of the reaction mechanism in differential form (Table 2).

An estimation of the activation energy can be obtained using the Arrhenius's equation [9].

$$k = A \exp\left(\frac{-E}{RT}\right) \quad (9)$$

where A is the pre-exponential factor (min^{-1}). E is the activation energy (kJ mol^{-1}). R is the universal gas constant ($8.314 \text{ J K}^{-1} \text{ mol}^{-1}$), T is the absolute temperature (K) and t is the reaction time (min).

For a constant heating rate β during gasification, $\beta = dT/dt$, rearranging Eq. (8) and integrating by using the Coats-Redfern method [26] one obtains:

$$\ln \left[\frac{g(x)}{T^2} \right] = \ln \left[\frac{AR}{\beta E} \left(1 - \frac{2RT}{E} \right) \right] - \frac{E}{RT} \quad (10)$$

where $g(x)$ refers to the reasonable model of the reaction mechanism in integral form (Table 2).

It is obvious that for most values of E and for the temperature range of gasification, the expression $\ln[AR/\beta E(1 - 2RT/E)]$ in Eq. (10) is basically constant [27,28]. A straight line should be achieved when the left side of Eq. (10) is plotted versus $1/T$.

Moreover, if the conversion (x) is recalculated, the plot of left side of Eq. (10) versus $1/T$, a straight line with a high correlation coefficient of linear regression analysis should be given. The activation energy E can be determined from the slope of the line ($-E/R$) by taking the temperature at which $w_t = (w_i - w_f)/2$ in place of T in the intercepts term of Eq. (10) the pre-exponential factor A can also be calculated [28–31].

Table 3 – Activity indexes of non-catalytic and catalytic PC and SCB.

Sample	T_i (°C)	T_{\max} (°C)	T_f (°C)	$T_{0.5}$ (°C)	DTG_{\max} (–% min^{-1})
PC	815	1081	1180	1068	7.89
PC + 1%	780	1017	1138	998	7.15
PC + 3%	750	1005	1102	962	6.97
PC + 5%	743	980	1108	942	6.52
PC + 7%	724	948	1138	930	6.07
PC + 9%	737	980	1120	958	6.04
SCB [S1]	160	351	540	335	8.35
SCB [S2]	630	874	976	845	1.19
SCB + 5% [S1]	140	347	510	328	10.28
SCB + 5% [S2]	623	832	936	793	1.21

T_i and T_f are the initial and final gasification temperatures, respectively; $T_{0.5}$ is the temperature when carbon conversion ratio is 50%; T_{\max} is the temperature when gasification rate reaches the maximum; DTG_{\max} is the maximum rate of mass loss; S1 is the stage 1 and S2 is the stage 2.

Table 4 – Activity indexes of non-catalytic and catalytic [PC:SCB] at 5 wt% loading FeCl_3 .

Sample	Stage 1		Stage 2	
	1:1	[1:1] + 5% FeCl_3	1:1	[1:1] + 5% FeCl_3
T_i ($^{\circ}\text{C}$)	170	158	690	702
T_{\max} ($^{\circ}\text{C}$)	342	332	1078	986
T_f ($^{\circ}\text{C}$)	445	337	1242	1148
$T_{0.5}$ ($^{\circ}\text{C}$)	336	288	1051	920
DTG_{\max} ($-\% \text{ min}^{-1}$)	3.68	3.40	3.72	3.14

T_i and T_f are the initial and final gasification temperatures, respectively; $T_{0.5}$ is the temperature when carbon conversion ratio is 50%; T_{\max} is the temperature when gasification rate reaches the maximum; DTG_{\max} is the maximum rate of mass loss.

The function $g(x)$ depends on the mechanism controlling the reaction, size and shape of the reacting particles. The function $g(x)$ for the basic model employed for the kinetic study of solid-state reactions is shown in Table 2.

3. Results and discussion

3.1. Thermal behaviour, carbon conversion and reactivity analyses

Fig. 1 shows the experimental TG and DTG curves for non-catalytic and catalytic gasification of PC with FeCl_3 catalyst at different concentrations (0–9 wt%). It can be observed that the non-catalytic and catalytic PC gasification took place almost completely in one-stage process (char gasification stage) at a higher temperature ($>650^{\circ}\text{C}$) as it was observed by the presence of only one peak in DTG curve. It was found that there was a lateral shift for the minimum rate of mass loss and its corresponding temperature when the FeCl_3 concentration was increased from 0 to 7 wt%. Addition of 7 wt% FeCl_3 gives the lowest minimum rate of mass loss and its corresponding temperature.

Table 3 presents the activity indexes of non-catalytic and catalytic of PC and SCB gasification. From Table 3 it can be noticed that the maximum rate of mass loss and its corresponding temperature were decreased randomly from $7.89\% \text{ min}^{-1}$; 1080°C for pure PC to $6.07\% \text{ min}^{-1}$; 948°C for PC with 7 wt% FeCl_3 and to $6.04\% \text{ min}^{-1}$; 980°C for PC with 9 wt% FeCl_3 . It was found that the maximum rate of mass loss and its corresponding temperature are inversely proportional to the concentration of FeCl_3 . It is concluded that the thermal behaviour of PC was significantly affected by the loading of FeCl_3 .

The experimental TG and DTG curves of non-catalytic and catalytic (FeCl_3 at 5 wt% concentration) of SCB and the blend are shown in Fig. 2. It seems that the gasification of SCB and the blend occurred in two stages (pyrolysis and char gasification). The first weight loss (stage 1) occurred at the equivalent temperature ($<500^{\circ}\text{C}$), whereas the shape and position on the time axis of these peaks are essentially the same. The last stage of mass loss (stage 2) took place at a higher temperature ($>600^{\circ}\text{C}$). The loss in stage 1 would be attributed to volatile matter released from the decompositions of hemicellulose and cellulose, while stage 2 would be due to the char gasification. It was found that FeCl_3 has a less significant effect on the gasification behaviour of SCB (pyrolysis stage) compared with the PC

and blend. Table 4 shows the activity indexes of non-catalytic and catalytic [PC:SCB] at 5 wt% FeCl_3 . It was found that the DTG_{\max} is directly proportional to SCB content in the pyrolysis stage. However, the opposite trend was obtained in the char gasification stage. In the pyrolysis stage the DTG_{\max} increased gradually from 8.35 min^{-1} for single SCB to 10.28 min^{-1} for SCB with 5 wt% FeCl_3 . While in char gasification stage the DTG_{\max} is almost the same and T_{\max} was decreased randomly from 874°C for pure SCB to 832°C for SCB with 5 wt% FeCl_3 .

The carbon conversion profiles of samples versus reaction time are presented in Fig. 3. While the reactivity index and its improvement (catalytic effects) of PC, SCB and blend are shown in Fig. 4. It was observed that the thermal stability of PC

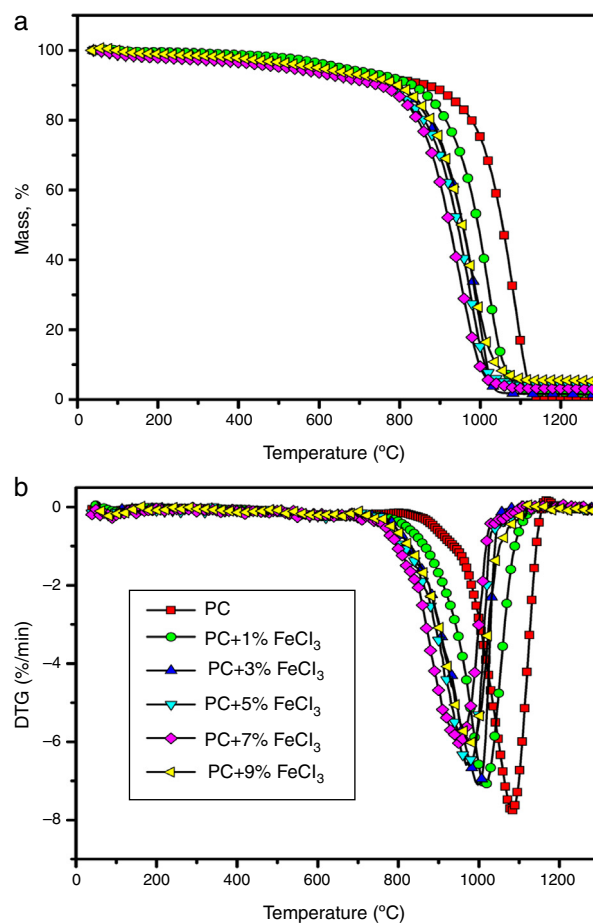


Fig. 1 – TG and DTG curves of non-catalytic and catalytic with FeCl_3 catalyst at different concentrations.

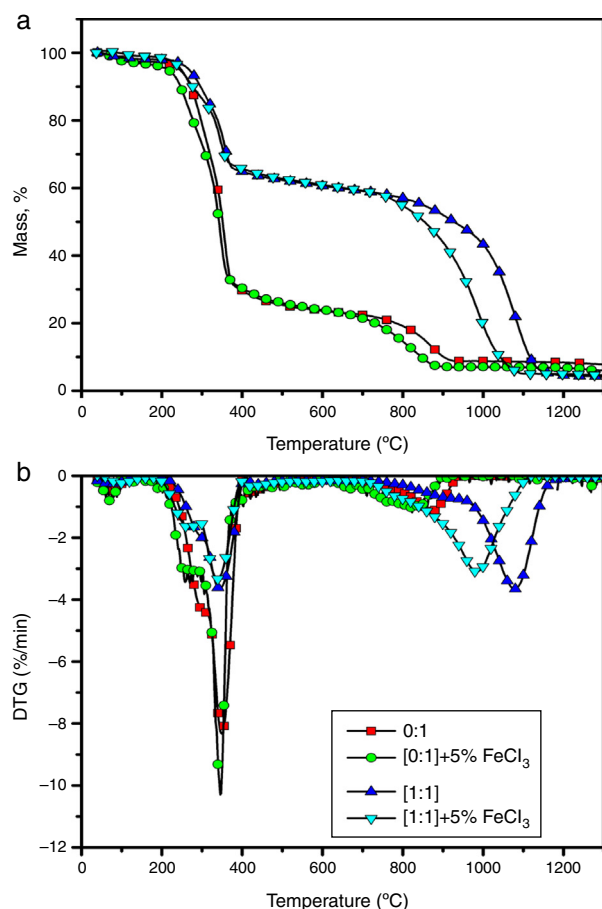


Fig. 2 – TG and DTG curves of non-catalytic and catalytic gasification of SCB and blend with FeCl₃ catalyst at 5 wt% concentration.

is very high, with almost no conversion occurring at temperatures lower than 1080 °C. This indicates that the petroleum coke was difficult to gasify, and the industrial non-catalytic gasification of petroleum coke generally requires temperature over 1080 °C.

It was found that the carbon conversions of PC, SCB and blend are significantly affected by the FeCl₃ loading and became less significant in the pyrolysis stage of pure SCB. From Fig. 3 it can be observed that the lowest required time for complete conversion was achieved at concentration of FeCl₃ 7 wt%. From Fig. 4, it was observed that the gasification reactivity increased gradually from 1.39 min⁻¹ at pure PC with FeCl₃ concentration increasing and reached the maximum value (2.19 min⁻¹) at 7 wt% FeCl₃ and then decreased to 1.93 min⁻¹ at 9 wt% FeCl₃. Since the volatile matter and ash content in PC are very low and fixed carbon is high, the conversion of pyrolysis is quite limited for the whole gasification process. Therefore, char gasification is the main step in the CO₂ gasification of PC. Such considerable reduction in the reactivity could be attributed to the localised deposition of FeCl₃ particles on the char surface and forming clusters. High concentration of FeCl₃ imposed inhibition either by blocking of accessible active sites on the char surface or deactivation of neighbouring FeCl₃ due to the formation

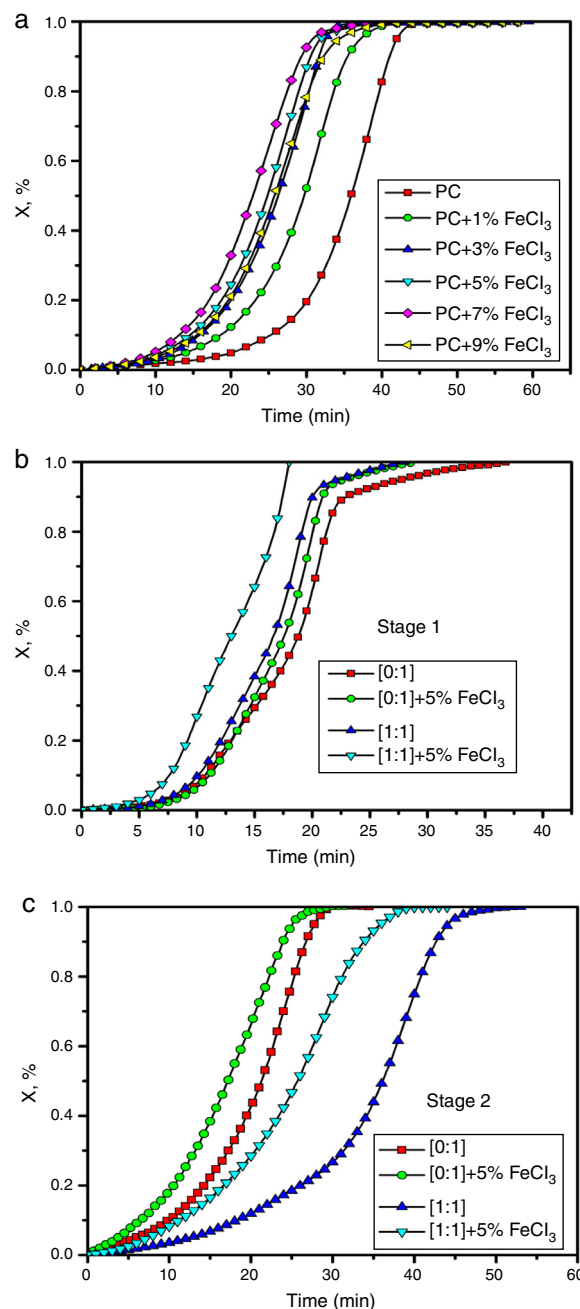


Fig. 3 – Conversion (x) versus time of non-catalytic and catalytic PC with FeCl₃ at different concentrations (a); non-catalytic and catalytic [SCB and blend] with FeCl₃ at 5 wt% at stage 1 (b) and stage 2 (c).

of agglomerates [23]. It is concluded that the PC reactivity was improved by 39.6% when 7 wt% of FeCl₃ was added to PC.

Also it was found that in the pyrolysis stage of SCB and blend the reactivity is higher than that in the char gasification stage. This could be attributed to a higher volatile matter and ash content in SCB besides the effect of FeCl₃ as catalysts. It was found that for char gasification stage of SCB and blend, the addition of 5 wt% FeCl₃ leads to improvements in their reactivities to 18.7% and 29.8%, respectively.

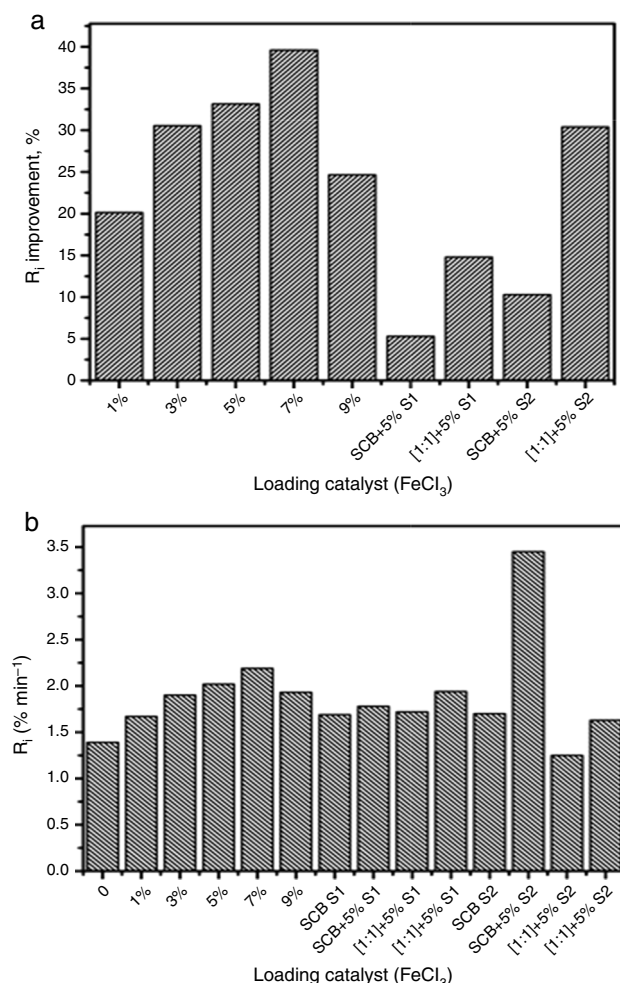


Fig. 4 – FeCl₃ effects (a) Reactivity index and (b) reactivity improvement.

3.2. Synergistic interactions analysis

The synergistic interactions might be due to a high reactivity of biomass and high volatile matter content in biomass. The synergy also mainly due to the catalysis of the alkali metal in SCB and PC, such as K, Mg and Ca as well as other alkali metals and alkaline earth metals (Fe) (refer to Table 1). They acted as a catalytic role and caused the interaction between the blend during the co-gasification process [2]. The comparison results of the experimental and calculated DTG curves of the non-catalytic and catalytic blend gasification with 5 wt% FeCl₃ are presented in Fig. 5. At both conditions (non-catalytic and catalytic) the deviations (interactions) in char stage of the blend were observed and the synergistic interactions became more significant in the pyrolysis stage. This could be due to the higher volatile matter, high alkali metals and alkaline earth metals in SCB and also due to the FeCl₃ effect. For non-catalytic blend gasification, slight interactions were observed at temperature regions of (986–1056 °C) and (1108–1160 °C). It is concluded that the synergistic interactions between the catalytic blended fuels (SCB with 5 wt%

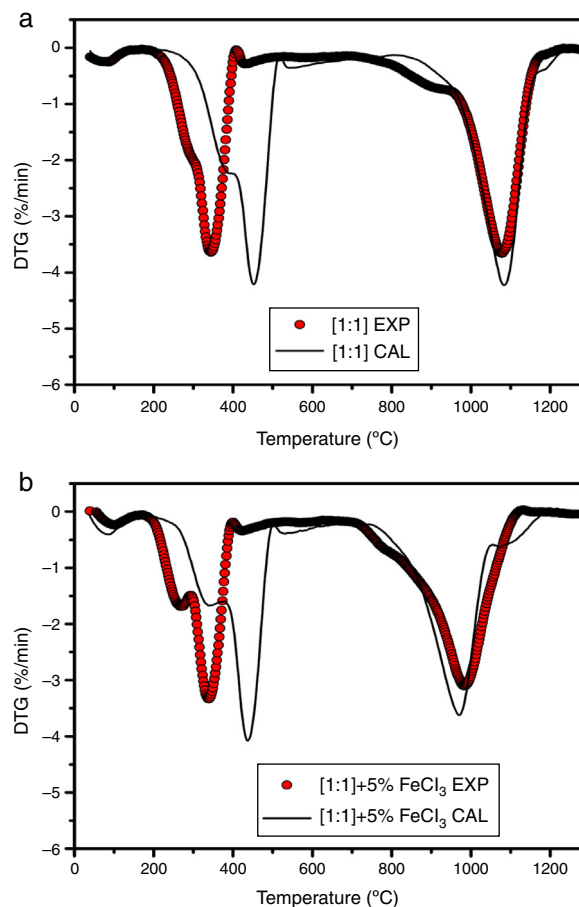


Fig. 5 – Synergetic effect between the blended fuels at (a) non-catalytic and (b) catalytic with FeCl₃ at 5 wt % concentration.

FeCl₃) are more significant as compared with the non-catalytic blends.

3.3. Kinetic analysis

The highest correlations coefficient was given by plotting $\ln[g(x)/T^2]$ versus $1/T$, which is presented in Fig. 6. The values of E and A were obtained from the slope of each line. The kinetic parameters results of non-catalytic and catalytic PC at different loading of FeCl₃ are given in Table 5, while the kinetic parameters results of non-catalytic and catalytic of SCB and blend at 5 wt% are listed in Table 6.

From Fig. 6 all models show higher values of R^2 (>0.98%) for all samples. However, the highest values were obtained by the models R_2 and R_3 . From the kinetic results of catalytic and non-catalytic of PC (Table 5) it was shown that for all models when the loading of FeCl₃ increases the values of E and A decreases gradually to reach minimum values at 7 wt% FeCl₃ and then slowly increases with the increasing loading of FeCl₃. While the opposite results were shown for the values of k . These results indicate that the catalysts have a significant effect on gasification reaction rate which confirms the results obtained in section (3.2). For all samples, the lowest (E and A) and highest k values were

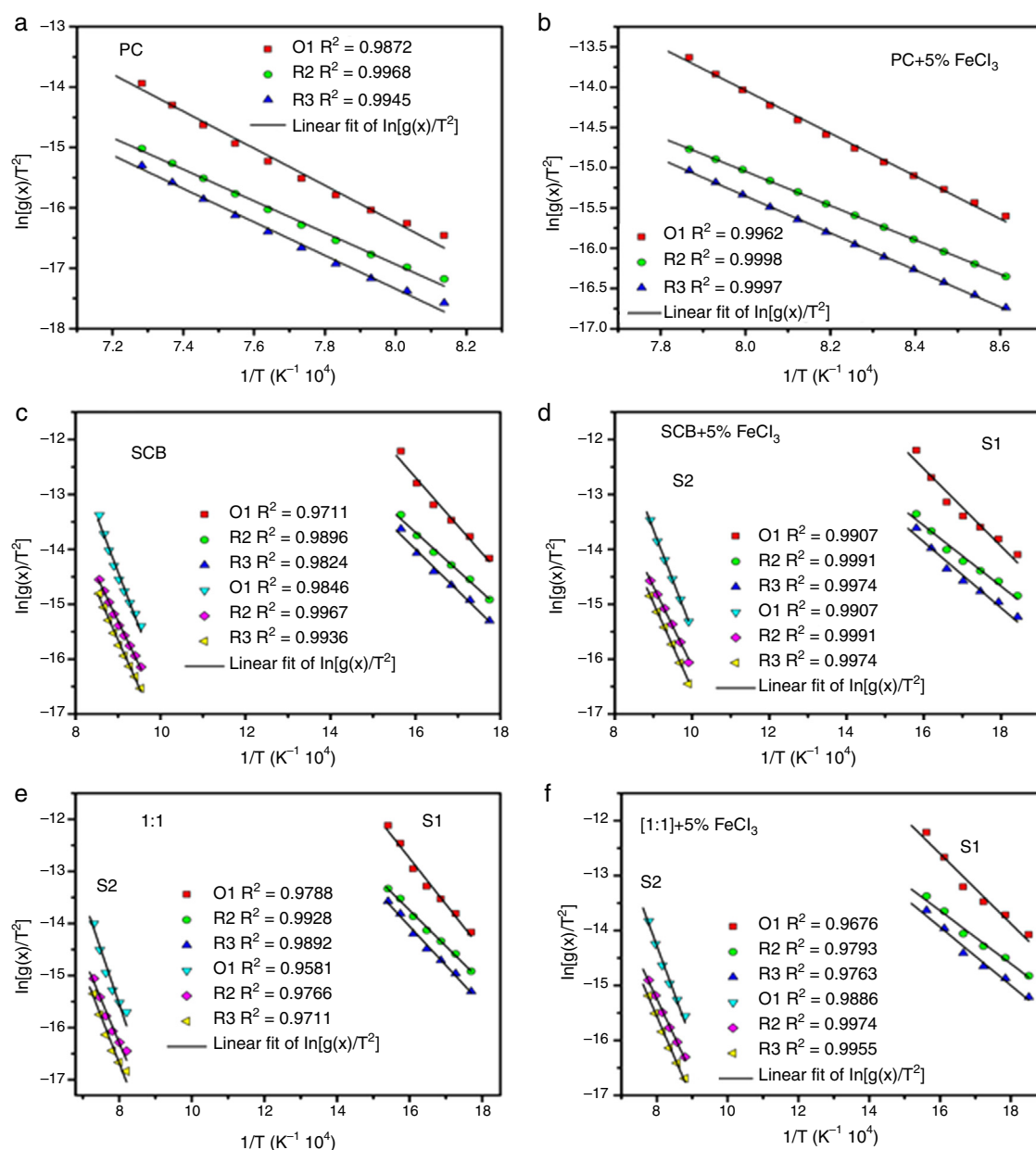


Fig. 6 – Plots of $\ln[g(x)/T^2]$ against $1/T$ for non-catalytic and catalytic of PC, SCB and blend with FeCl_3 at 5 wt% concentration.

achieved by the phase boundary controlled reactions model (R_2), however the opposite trends were obtained by the first order chemical reaction model O_1 . Table 7 lists the activation energies reduction during CO_2 catalytic gasification of samples.

From Table 7 it was observed that the lowest reduction of E is 29.12%, which was achieved by model R_2 at PC with 7 wt% FeCl_3 . Model R_2 is the optimum reaction mechanism for CO_2 catalytic and non-catalytic gasification of PC. It was established that the 7 wt% is the optimum concentration value for loading FeCl_3 into the PC because it gives the highest reactivity improvement and lowest activation energy reduction. For all the addition of 7 wt% FeCl_3 into PC, its activation energy decreases up to 22%. Zhou et al. [18] reported that 5 wt% FeCl_3 decreases the activation energy of PC up to 15%

during CO_2 gasification. However, in this study the addition of 5 wt% FeCl_3 decreased the activation energy of PC up to 19%. From Fig. 6, it was observed that for both reaction stages of SCB and blend, the models R_2 and R_3 show higher values of R^2 as compared with model O_1 . This means that the gasification of samples is chemically-controlled. The lowest R^2 value is 0.9581, which was obtained by model O_1 in the char gasification stage of blend. It was found that model R_2 was the most suitable one to describe the reactions. From Table 6 it was found that for both reaction stages of SCB and the blend, model R_2 shows the lowest values of E and A and highest values of k . The values of E and A in the pyrolysis stage are lower than the values in the char stage. However, higher values of k were obtained in the pyrolysis stage and lower values in the char stage. These could be due to the higher

Table 5 – Kinetic parameter of non-catalytic and catalytic PC at different loading FeCl₃.

Sample	PC	PC + 1%	PC + 3%	PC + 5%	PC + 7%	PC + 9%
<i>Model O₁</i>						
E	255.57	215.59	208.74	206.47	202.32	205.43
A	1.25E+11	9.12E+11	8.59E+10	8.41E+10	8.10E+10	8.33E+10
k	4.09E+02	6.31E+03	1.00E+04	1.17E+04	1.54E+04	1.26E+04
<i>Model R₂</i>						
E	218.12	182.20	177.43	175.11	170.32	172.69
A	9.32E+10	6.68E+10	7.82E+10	6.21E+10	5.91E+10	6.06E+10
k	5.32E+03	5.95E+04	1.00E+05	9.05E+04	1.30E+05	1.11E+05
<i>Model R₃</i>						
E	229.96	192.74	187.35	185.03	180.43	183.02
A	1.03E+11	7.41E+10	8.63E+10	6.87E+10	6.56E+10	6.73E+10
k	2.37E+03	2.94E+04	5.18E+04	4.93E+04	6.56E+04	5.63E+04

E (kJ mol⁻¹), A (min⁻¹), k (min⁻¹).**Table 6 – Kinetic parameter of non-catalytic and catalytic SCB, PC:SCB blend at 5 wt% loading FeCl₃.**

Sample	Stage 1			Stage 2		
	E	A	k	E	A	k
<i>Model O₁</i>						
0:1	73.25	1.44E+10	5.31E+07	168.52	5.79E+10	1.47E+05
[0:1] + 5%	58.57	1.07E+10	1.21E+08	152.06	4.81E+10	4.29E+05
1:1	73.41	1.44E+10	5.31E+07	171.91	6.01E+10	1.17E+05
[1:1] + 5%	52.85	9.54E+09	1.67E+08	145.98	4.47E+10	6.35E+05
<i>Model R₂</i>						
0:1	58.06	1.06E+10	1.25E+08	134.87	3.89E+10	1.29E+06
[0:1] + 5%	45.85	8.43E+09	2.53E+08	120.42	3.19E+10	3.19E+06
1:1	57.33	1.04E+10	1.31E+08	138.70	4.09E+10	1.01E+06
[1:1] + 5%	40.16	1.14E+10	5.27E+08	114.90	2.95E+10	4.50E+06
<i>Model R₃</i>						
0:1	62.81	1.16E+10	9.61E+07	145.43	4.44E+10	6.58E+05
[0:1] + 5%	49.82	9.01E+09	1.99E+08	130.34	3.66E+10	1.72E+06
1:1	62.31	1.15E+10	9.83E+07	149.14	4.65E+10	5.18E+05
[1:1] + 5%	44.12	1.16E+10	3.99E+08	124.62	3.39E+10	2.46E+06

E (kJ mol⁻¹), A (min⁻¹), k (min⁻¹).

volatile matter, high alkali metals and alkaline earth metals in SCB and also due to the addition of FeCl₃ to SCB and the blend.

From Table 7 the highest values of E reduction during the CO₂ catalytic gasification of SCB and the blend were achieved by model R₂. It seems that the addition of 5 wt% FeCl₃ leads to

higher reduction of E by (24.08 and 29.95%) for pyrolysis stage of SCB (10.71 and 17.16%) for char gasification stages of the blend. For both catalytic and non-catalytic CO₂ gasification, the activation energies of mixed fuels obtained by all models were lower than the average value of the individual fuels. This confirms the existence synergistic interaction during the co catalytic CO₂ gasification. Finally, all the models based on Coats–Redfern method were successfully utilised to describe the reactive behaviour and predict the reaction mechanism of CO₂ catalytic gasification of samples followed the order model R₂ > R₃ > O₁.

Table 7 – Activation energy (E) reduction (%) during CO₂ catalytic gasification (catalytic effects).

Sample	Model O ₁	Model R ₂	Model R ₃
PC + 1%	15.64	16.47	16.19
PC + 3%	18.32	18.65	18.53
PC + 5%	19.21	19.72	19.54
PC + 7%	20.84	21.91	21.54
PC + 9%	19.62	20.83	20.41
SCB + 5% S1	19.84	24.08	22.92
SCB + 5% S2	9.77	10.71	10.38
[1:1] + 5% S1	28.01	29.95	29.19
[1:1] + 5% S2	15.08	17.16	16.44

4. Conclusions

PC gasification under non-catalytic and catalytic conditions took place, almost completely in one-stage (char gasification stage) at higher temperature (>700 °C). The carbon conversions of PC, SCB and the blend were significantly affected by the FeCl₃. Among various catalyst loadings 7 wt% FeCl₃ had the highest impact on the PC gasification reactivity

enhancement and reduction of activation energy. On the other hand, for char gasification stage of SCB and blend, the addition of 5 wt% FeCl_3 leads to improve their reactivities to 18.7% and 29.8%, respectively. The loading FeCl_3 has a less significant effect on the gasification behaviour of SCB (pyrolysis stage) as compared with the PC and blend. For both conditions the synergistic interactions in char stage of the blend were observed and it became more significant in the pyrolysis stage. It was found that the synergistic interaction between the PC and SCB during catalytic gasification (SCB with 5 wt% FeCl_3) was more significant as compared with the non-catalytic blend gasification. Activation energy of 7 wt% FeCl_3 loaded PC was obtained by model R_2 , as $208.01 \text{ kJ mol}^{-1}$, which was $82.11 \text{ kJ mol}^{-1}$ lower than that of non-catalysed PC. The results show that for both catalytic and non-catalytic CO_2 gasification, the activation energies of mixed fuels obtained by all the models were lower than the average value of the individual fuel. This confirms the existence synergistic interaction during the co catalytic CO_2 gasification. Finally, all the models succeeded in describing the thermal behaviour and predicting the reaction mechanism of non-catalytic and catalytic CO_2 gasification of PC and SCB in the following order: $R_2 > R_3 > O_1$.

Conflicts of interest

The authors declare no conflicts of interest.

Acknowledgements

The authors gratefully acknowledge the extended help from the Analytical and Testing Centre of Huazhong University of Science and Technology.

REFERENCES

- [1] Edreis E, Luo G, Li A, Chao C, Hu H, Zhang S, et al. CO_2 co-gasification of lower sulphur petroleum coke and sugar cane bagasse via TG-FTIR analysis technique. *Bioresour Technol* 2013;136:595–603.
- [2] Edreis EMA, Luo G, Li A, Xu C, Yao H. Synergistic effects and kinetics thermal behaviour of petroleum coke/biomass blends during H_2O co-gasification. *Energy Convers Manag* 2014;79:355–66.
- [3] Li Y, Yang H, Hu J, Wang X, Chen H. Effect of catalysts on the reactivity and structure evolution of char in petroleum coke steam gasification. *Fuel* 2014;117:1174–80.
- [4] Bayram A, Müezzinoğlu A, Seyfioğlu R. Presence and control of polycyclic aromatic hydrocarbons in petroleum coke drying and calcination plants. *Fuel Process Technol* 1999;60:111–8.
- [5] Gao C, Vejehati F, Katalambula H, Gupta R. Co-gasification of biomass with coal and oil sand coke in a drop tube furnace. *Energy Fuels* 2009;24:232–40.
- [6] Nemanova V, Abedini A, Liliedahl T, Engvall K. Co-gasification of petroleum coke and biomass. *Fuel* 2014;117:870–5.
- [7] Zou JH, Zhou ZJ, Wang FC, Zhang W, Dai ZH, Liu HF, et al. Modeling reaction kinetics of petroleum coke gasification with CO_2 . *Chem Eng Process: Process Intensif* 2007;46:630–6.
- [8] Yoon SJ, Choi YC, Lee SH, Lee JG. Thermogravimetric study of coal and petroleum coke for co-gasification. *Korean J Chem Eng* 2007;24:512–7.
- [9] Ahmed II, Gupta AK. Sugarcane bagasse gasification: global reaction mechanism of syngas evolution. *Appl Energy* 2012;91:75–81.
- [10] Mothé CG, de Miranda IC. Characterization of sugarcane and coconut fibers by thermal analysis and FTIR. *J Therm Anal Calorim* 2009;97:661–5.
- [11] Edreis E, Luo G, Yao H. Investigations of the structure and thermal kinetic analysis of sugarcane bagasse char during non-isothermal CO_2 gasification. *J Anal Appl Pyrolysis* 2014;107:107–15, <http://dx.doi.org/10.1016/j.jaap.2014.02.010>.
- [12] Nsáful F, Görgens J, Knoetze J. Comparison of combustion and pyrolysis for energy generation in a sugarcane mill. *Energy Convers Manag* 2013;74:524–34.
- [13] Alonso Pippo W, Garzone P, Cornacchia G. Agro-industry sugarcane residues disposal: the trends of their conversion into energy carriers in Cuba. *Waste Manag* 2007;27:869–85.
- [14] Monterroso R, Fan M, Zhang F, Gao Y, Popa T, Argyle MD, et al. Effects of an environmentally-friendly, inexpensive composite iron-sodium catalyst on coal gasification. *Fuel* 2014;116:341–9.
- [15] Wang J, Yao Y, Cao J, Jiang M. Enhanced catalysis of K_2CO_3 for steam gasification of coal char by using $\text{Ca}(\text{OH})_2$ in char preparation. *Fuel* 2010;89:310–7.
- [16] Popa T, Fan M, Argyle MD, Slimane RB, Bell DA, Towler BF. Catalytic gasification of a Powder River Basin coal. *Fuel* 2013;103:161–70.
- [17] Popa T, Fan M, Argyle M, Dyar M, Gao Y, Tang J, et al. H_2 and CO generation from coal gasification catalyzed by a cost-effective iron catalyst. *Appl Catal A: Gen* 2013;464:207–17.
- [18] Zhou Z-j, Hu Q-j, Liu X, Yu G-s, Wang F-c. Effect of iron species and calcium hydroxide on high-sulfur petroleum coke CO_2 gasification. *Energy Fuels* 2012;26:1489–95.
- [19] Lahijani P, Zainal ZA, Mohamed AR. Catalytic effect of iron species on CO_2 gasification reactivity of oil palm shell char. *Thermochim Acta* 2012;546:24–31.
- [20] Di Blasi C. Combustion and gasification rates of lignocellulosic chars. *Prog Energy Combust Sci* 2009;35:121–40.
- [21] Haykiri-Acma H, Yaman S. Interaction between biomass and different rank coals during co-pyrolysis. *Renew Energy* 2010;35:288–92.
- [22] Xu C, Hu S, Xiang J, Zhang L, Sun L, Shuai C, et al. Interaction and kinetic analysis for coal and biomass co-gasification by TG-FTIR. *Bioresour Technol* 2014;154:313–21.
- [23] Lahijani P, Zainal ZA, Mohamed AR, Mohammadi M. CO_2 gasification reactivity of biomass char: catalytic influence of alkali, alkaline earth and transition metal salts. *Bioresour Technol* 2013;144:288–95.
- [24] Lahijani P, Zainal ZA, Mohamed AR, Mohammadi M. Ash of palm empty fruit bunch as a natural catalyst for promoting the CO_2 gasification reactivity of biomass char. *Bioresour Technol* 2013;132:351–5, <http://dx.doi.org/10.1016/j.biortech.2012.10.092>.
- [25] Zhan X, Jia J, Zhou Z, Wang F. Influence of blending methods on the co-gasification reactivity of petroleum coke and lignite. *Energy Convers Manag* 2011;52:1810–4.
- [26] Coats A, Redfern J. Kinetic parameters from thermogravimetric data. *Nature* 1964;201:68–9.
- [27] Gong C, PiWen H, Bo X, ZhiQuan H, ShiMing L, LeGuan Z, et al. Gasification of biomass micron fuel with oxygen-enriched air: thermogravimetric analysis and gasification in a cyclone furnace. *Energy (Oxford)* 2012;43:329–33.

- [28] Çepelioğullar Ö, Pütün AE. Thermal and kinetic behaviors of biomass and plastic wastes in co-pyrolysis. *Energy Convers Manag* 2013;75:263–70.
- [29] Gil M, Casal D, Pevida C, Pis J, Rubiera F. Thermal behaviour and kinetics of coal/biomass blends during co-combustion. *Bioresour Technol* 2010;101:5601–8.
- [30] Zhou L, Wang Y, Huang Q, Cai J. Thermogravimetric characteristics and kinetic of plastic and biomass blends co-pyrolysis. *Fuel Process Technol* 2006;87:963–9.
- [31] Cai J, Wang Y, Zhou L, Huang Q. Thermogravimetric analysis and kinetics of coal/plastic blends during co-pyrolysis in nitrogen atmosphere. *Fuel Process Technol* 2008;89:21–7.